Prediction of Diffuse Axonal Injury with a Strain Measure from an Analytical Model

Hong Zou and James P. Schmiedeler

ABSTRACT

Diffuse axonal injury (DAI) is one of the most devastating types of traumatic brain injury and frequently occurs from automobile crashes. Strain deformation induced by shear force from sudden acceleration of the human head during impact has been recognized as a major cause of DAI. Recent mathematical studies on strain damage of brain tissue are dominated by finite element (FE) modeling work. Although offering detailed modeling of anatomical structures, FE models have not been fully validated due to the lack of complete knowledge of the material properties of brain tissue. Based on a well-established analytical brain injury model, which was validated against the most advanced experimental brain motion data and compared with high-fidelity FE results under low-severity impacts, a measure of strain for DAI prediction is presented. Increasing with higher accelerations under more severe impact, the maximum shear strain was selected as the injury indicator of DAI because DAI most likely results from shear force. This strain measure was applied to the frontal crash tests using the acceleration data collected with dummies through the New Car Assessment Program (NCAP) conducted by the National Highway Traffic Safety Administration (NHTSA). The results were compared with the Head Injury Criterion (HIC) and the Cumulative Strain Damage Measure (CSDM) in the SIMon FE head model developed by NHTSA. It shows that the simple measure of strain has the capabilities of predicting brain injuries from automobile crashes. The maximum shear strain from the analytical model can be used as a critical element to predict DAI. Including both linear and angular accelerations, this analytical model tends to fill the gap between HIC and the more complex SIMon, where HIC predicts injuries based only on linear accelerations while the SIMon prediction is dominated by angular accelerations.

INTRODUCTION

Recognized as a major public health problem, injuries resulting from transportation-related accidents are the most frequent type of personal injuries. According to the CDC Injury Research Agenda (2002), automobile crashes resulted in 40,965 deaths in 1999 and were the leading cause of death in the United States among people ages 1 to 34. Among all types of injuries, brain injury is the type most likely to result in death or permanent disability. The CDC (2005) estimates that 1.4 million people sustain a traumatic brain injury (TBI) and 50,000 die because of TBI each year in the USA. The cost of TBI totaled an estimated $56.3 billion in the U.S. in 1995 (Thurman et al., 1999), reflecting substantial impacts on individuals, families, and society. This presents a critical need for more effective ways to prevent brain injuries in automobile crashes.

Occurring over a more widespread area than focal brain injury, diffuse axonal injury (DAI) is one of the most devastating types of TBI and is the most significant cause of morbidity in patients with TBI. Strain deformation induced by shear force from sudden acceleration or deceleration of the head during impact has been recognized as a major cause of DAI, resulting in tearing axons, which lose the capability of transferring messages between neurons. However, further studies are needed to fully understand the mechanisms of DAI. Various experimental tests and mathematical models have been employed in the past decades to understand the mechanisms of DAI for better injury prediction and prevention.

Experiments have been conducted for years to study strain damage of the brain under impacts. Based on the experimental data on primates, Margulies and Thibault (1992) concluded that strains ranging from 0.05 to 0.10 correspond to moderate-to-severe DAI. Bain and Meaney (2000) conducted experiments by stretching right optic nerves of an adult guinea pig to produce axonal injuries. They found that functional impairment occurs at a threshold of 0.18 Lagrangian strain. Morrison III et al. (2003) used a hippocampal slice of a Wistar rat brain to study the tissue-level tolerance criterion. They suggested that a tissue Lagrangian strain of 0.20 may be a transition between non-injurious and injurious loads dependent on strain rates, which probably lies between 10 and 50 s^{-1}. Bayly et al. (2005) measured brain deformation in human volunteers under mild occipital deceleration. The strains were typically 0.02-0.05 during these mild impacts. In general, these studies suggest that the threshold of strain causing brain injury lies between 0.15 and 0.20 depending on different strain rates.

Recent mathematical studies on strain damage of brain tissue are dominated by finite element (FE) modeling work. Zhang et al. (2001) compared brain responses under frontal and lateral impacts using a three-dimensional FE head model. They found that the strain experienced in the brain tissue due to lateral impact is much higher. Takhounts and Eppinger (2003) developed the SIMon FE head model to predict various brain injuries due to impact based on a three-dimensional FE model originally developed by Bandak and Eppinger (1994) and later improved by DiMasi et al. (1995). Although offering detailed modeling of anatomical structures, these FE models have not been fully validated due to the lack of complete knowledge of the complex material properties and interface conditions of the human head.

Lumped-parameter models have also been used to study head/brain injuries under impacts. Slattenschek and Tauffkirchen (1970) developed a translational model consisting of two masses connected

by a spring and a damper in parallel to evaluate head injuries during impacts. This model was used and modified by other researchers to study head injuries (Brinn and Staffeld, 1970; Stalnaker et al., 1971). Low's (1986) pure rotational head injury model consisting of three masses connected by eight springs and dampers was not validated due to the lack of experimental data. Including both linear and angular head kinematics as inputs, Alem's (1974) twelve-degree-of-freedom head model is too complex. More recently, Young (2003) developed an analytical model for predicting the responses of a fluid-filled shell impacting a solid sphere. However, none of those lumped-parameter models has a validated measure for brain injury prediction under impacts.

Therefore, based on a recently developed analytical brain injury model, which was validated against the most advanced experimental brain motion data and compared with high-fidelity FE results under low-severity impacts, a measure of strain for DAI prediction is presented in this work. The objective of this study is to validate the proposed strain measure and evaluate its capabilities of brain injury prediction in more severe, realistic crash tests.

MODEL DEVELOPMENT

This work proposes a simple measure of strain based on a lumped-parameter human brain injury model that can be dealt with analytically for DAI prediction under impacts. Based upon the knowledge from the literature, the development of the analytical model operates from a fundamental assumption that the translational and rotational motions of the brain with respect to the skull are coupled. A planar model is adequate to capture the important characteristics of brain motion since relative brain motion is primarily planar, even for three-dimensional head kinematics, according to Hardy et al. (2001).

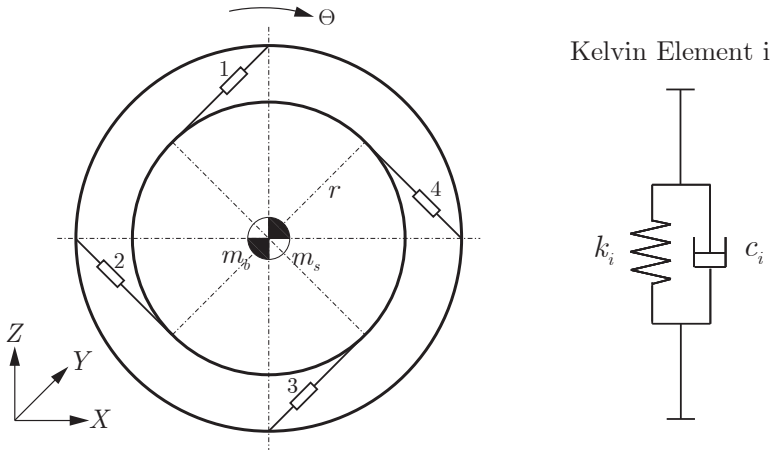

Figure 1: Schematic of the human brain injury model.

Fully described in Zou et al. (2006), a lumped-parameter model that captures the motion of the human head in the sagittal plane has been developed, as shown in Figure 1. The model consists of

a circular skull and brain having masses, m_s and m_b, and moments of inertia, I_s and I_b, where the subscripts "s" and "b" indicate the skull and brain, respectively. The skull and brain are connected by four Kelvin elements, each having a spring constant k_i and a damping coefficient c_i, where $i = 1 - 4$. The centers of mass of the skull and the brain are assumed to be coincident at the geometric center. In the neutral position, each Kelvin element makes a 45-degree angle with the horizontal and is attached to the brain at a perpendicular offset distance of r with respect to the center of mass. The parameter r is also the radius of the circular brain. The radius of the circular skull is then given according to the geometry. The validation of the model against the experimental brain motion data is presented in detail in the previous study (Zou et al., 2006).

Based on this analytical brain injury model, which was compared with high-fidelity FE results under low-severity impacts, a measure of strain for DAI prediction is proposed here. The brain is assumed spherical although its motion is limited within the sagittal plane. The brain is divided into two hemispheres with a horizontal cross section passing through the center of gravity of the whole brain. The upper hemispherical brain is used to develop the strain measure. Strain profile on the base of the hemisphere is used as the strain measure in the brain tissue. The shear and normal forces acting on the base of the hemisphere are assumed to be evenly distributed and concentrated at the center of the base for simplicity of analysis. Note that the rotation of the brain is indeed partially caused by unevenly distributed forces on the base.

The shear force and the normal force can be derived with the known brain kinematics and time history of the forces in the Kelvin elements. The area of the base of the hemisphere is estimated using the averaged dimension of the human brain in the literature, so the shear stress and normal stress can be calculated. For simplicity, the brain is modeled as linear elastic material, as many FE human head models adopted (Ward and Chan, 1980; Hosey and Liu, 1982; Khalil and Viano, 1982; Ruan et al., 1991; Zhou et al., 1995; Claessens et al., 1997). With carefully selected Young's modulus E and Poisson ratio ν of the brain tissue, the shear strain and normal strain on the base can be obtained.

PARAMETER SELECTION

The material properties of the brain tissue are needed to calculate the strains, while other parameters, such as the spring and damping constants, have already been chosen in the previous study (Zou et al., 2006). By applying experimentally measured head kinematics to the model, the normal strain and shear strain in the brain tissue are computed using the proposed scheme. The brain material properties are selected to best represent the severity of impact.

Linear elastic brain tissue is used in this model to calculate strains in the brain during impact. However, the value of the Young's modulus of the brain tissue varies in a large range in the literature. Morrison III et al. (2003) assumed the brain tissue to be linearly elastic with a Young's modulus of 10 KPa in their finite element model to predict the strain field in a stretched culture of rat brain tissue. Galford and McElhaney (1970) obtained an elastic modulus of 66.7 KPa in their human brain vibration tests. This value was widely adopted as the linear elastic modulus in many FE models with linear elastic material constitutive laws (Ward and Chan, 1980; Hosey and Liu, 1982; Khalil and Viano, 1982; Ruan et al., 1991). Ueno et al. (1995) used 80.0 KPa as the Young's

Table 1: Material property of linear elastic brain tissue used in the literature.

Authors	Young's Modulus $E\,(KPa)$	Poisson Ratio ν
Morrison III et al., 2003	10	0.4999
Ward & Chan, 1980	66.7	0.49-0.4999
Hosey & Liu, 1982	66.7	0.48
Khalil & Viano, 1982	66.7	0.45-0.499
Ruan et al., 1991	66.7	0.48
Ueno et al., 1995	80.0	0.49
Chu et al., 1994	250	0.49
Huang et al., 1999, 2000	250	0.49
Willinger et al., 1999	675	0.48
Claessens et al., 1997	1000	0.48

modulus of the brain in their finite element model. In Chu et al's (1994) and Huang et al's (1999; 2000) work, they used 250 KPa as the Young's modulus in their finite element models to study brain injuries. The Young's modulus of the brain tissue is as large as 675 KPa in Willinger et al's (1999) work and 1000 KPa in Claessens et al's (1997) work. The Young's modulus of the brain tissue in the literature is summarized in Table 1.

By applying the head kinematics measured in Hardy et al's (2001) tests in Table 2, the normal strain and shear strain in the brain tissue are calculated. The maximum shear strain is selected as the indicator of strain measurement since shear strain has a larger magnitude than normal strain in each of the six tests. It is also consistent with the fact that DAI most likely results from shear force and shear deformation experienced in the brain. In order to have the strain calculation best represent the severity of impact and therefore, severity of brain injury, the Young's modulus E of the brain tissue is chosen as 150 KPa, which falls within the range of reported data. This selected Young's modulus of the linear elastic brain tissue is expected to narrow down the wide range of the brain material properties used in the literature. The Poisson ratio ν is chosen as 0.49 since the brain tissue is nearly incompressible.

As listed in Table 2, the magnitudes of maximum shear strain are consistent with the relative HIC15 values and the maximum resultant linear and angular accelerations. Test C755-T5 has the lowest maximum shear strain, the lowest HIC15 value, and the smallest magnitudes of the maximum linear and angular accelerations among all six tests. For test C383-T4, the highest maximum shear strain matches the highest HIC15, maximum linear acceleration, and maximum angular acceleration. In general, the maximum shear strain for Hardy et al's (2001) tests falls within the range of 0.04-0.14, which is reasonable compared with strain of magnitude 0.02-0.05 observed by Bayly et al. (2005) using human volunteers under occipital deceleration impacts and with the published threshold of strain, 0.15-0.20. The maximum shear strain in each individual test matches closely the severity of impact, which is characterized by the HIC15 and maximum resultant accelerations. Therefore, the maximum shear strain can be used as the injury indicator

Table 2: Comparing the maximum shear strain from the analytical model with the test configuration for all of the six tests in Hardy et al's (2001) work.

Test No.	Maximum Shear Strain	HIC15	Maximum Resultant Linear Acceleration (g)	Maximum Resultant Angular Acceleration $\left(rad/s^2\right)$
C755-T2	0.08	16.9	21.8	1753.2
C755-T3	0.07	21.3	24.4	1948.7
C755-T5	0.04	5.2	12.1	803.9
C383-T1	0.10	46.6	62.2	2745.7
C383-T3	0.12	67.6	62.4	3033.3
C383-T4	0.14	163.7	107.7	22393.9

for DAI prediction.

APPLICATION IN REAL CRASH TESTS

The strain measure predicts closely the severity of impact in Hardy et al's (2001) tests under low-severity impacts. To further evaluate its capabilities of DAI prediction, the proposed strain measure of the analytical brain injury model is applied to more severe, real crash tests in the New Car Assessment Program (NCAP) conducted by the National Highway Traffic Safety Administration (NHTSA). Frontal crash tests are selected since the impacts are primarily in the sagittal plane, wherein the analytical model lies. Recent crash tests are chosen such that their HIC15 values spread across a large range, representing impacts of various severity.

Anthropomorphic test devices (ATDs), mostly Hybrid III dummies, are seated in the vehicle to record the head kinematics during crash tests in NCAP. For head injury prediction, a 3-2-2-2 nine accelerometer package (NAP) is fully instrumented inside the dummy headform to measure nine linear accelerations at the center of gravity of the headform. The nine linear accelerations can be transformed to calculate three orthogonal angular accelerations, which fully describe the kinematics of the dummy head together with three linear accelerations. The formulation derived in Padgaonkar et al's (1975) work is used to calculate the angular accelerations from nine linear accelerations. The linear and angular accelerations of the head are then applied to the analytical model as inputs to compute the maximum shear strain in the brain tissue for injury prediction.

The crash tests are also reconstructed in the SIMon FE head model using the experimental data in NHTSA's vehicle crash test database. SIMon has detailed anatomical structures and was validated against experimental data collected in tests on cadavers and animals. It predicts brain injuries using three types of injury metrics: cumulative strain damage measure (CSDM), dilatational damage measure (DDM), and relative motion damage measure (RMDM). The results of strain measure in this study are compared with the HIC system and the SIMon model to evaluate their individual advantages and disadvantages for brain injury prediction.

RESULTS

Table 3 in the Appendix shows the configuration of 40 frontal crash tests in NCAP. The first four digits in the first column of Table 3 are the test number assigned by NHTSA. The two digits following the dashed line indicate dummy location on driver or passenger seat. For example, "01" represents driver, and "02" represents passenger. All of these frontal crash tests have an impact speed of about 56.3 kph (35 mph). Note that one crash test here explicitly means one set of acceleration data of the head collected with one ATD.

The headform kinematics collected with Hybrid III dummies in NHTSA's NCAP crash tests are listed in Tables 4 and 5 in the Appendix. The maximum absolute values of the accelerations and velocities in all of the three directions are listed. In the FE model, Kleiven (2005) concluded that the peak change in angular velocity had the best correlation with the principal strain in the brain tissue under a purely rotational impulse. It suggests that peak angular velocity is an important metric of brain injury during impacts. Most of the ATDs in frontal crash tests have dominant head kinematics in the sagittal plane, so this model is adequate to capture the key characteristics of the head response.

Sorted by the maximum shear strain, Figure 2 plots the maximum shear strain from the analytical model and the HIC15 values. For all of the 40 frontal crash tests, the HIC15 values are lower than the injury threshold of 700 except one test, 3952-02. Because linear kinematics are considered to be injurious to the brain and higher HIC15 implies larger linear kinematics, the analytical model in the sagittal plane is expected to yield relatively high maximum shear strain for the tests having HIC15 higher than 500. However, the analytical model yields a maximum shear strain of only 0.11 for test 4899-01 having a HIC15 of 544 because test 4899-01 has relatively small angular head kinematics. Contrarily, for test 5092-02 having a HIC15 of only 144, the analytical model produces a higher maximum shear strain of 0.14 due to the relatively large angular kinematics in 5092-02. In general, the analytical model produces relatively high shear strain for all the tests having HIC15 lower than 200 because of the combined linear and angular head kinematics, which are both treated as injurious inputs.

Also sorted by the maximum shear strain, Figure 3 compares the maximum shear strain from the analytical model with the CSDM in SIMon, which correlates to DAI. In the SIMon FE head model, Takhounts et al. (2003) selected 0.15 strain level as a critical value causing brain damage. A 25% volume of the whole brain experiencing strain over 0.15 is used as a preset "survivability" for cumulative strain damage. Having a HIC15 of 287, test 4081-02 is the only one that exceeds the preset CSDM threshold value of 25% in SIMon. However, it does not have a very high maximum shear strain (only 0.11) in the analytical model because the out-of-sagittal-plane kinematics are dominant in test 4081-02. It suggests that the planar model is limited to capture only in-plane characteristics of brain motion. Since test 4899-01 has very small angular head kinematics, SIMon gives a very small CSDM value of 0.53%, while the analytical model produces a relatively high maximum shear strain of 0.11 because of the linear head kinematics. For all of the tests having small angular head kinematics, SIMon predicts low CDSM values, while the analytical model generally does not follow the same trend becasue the linear head kinematics are also included as injurious inputs in the analytical model.

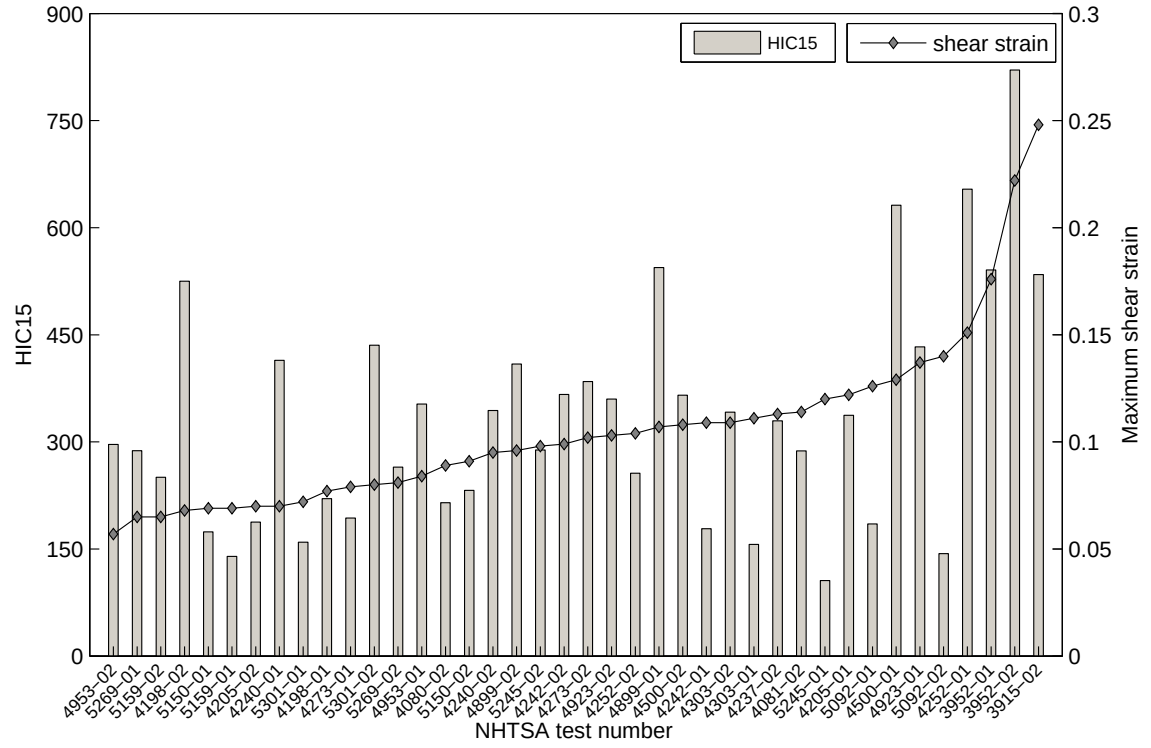

Figure 2: Comparison of the maximum shear strain from the analytical model and HIC15.

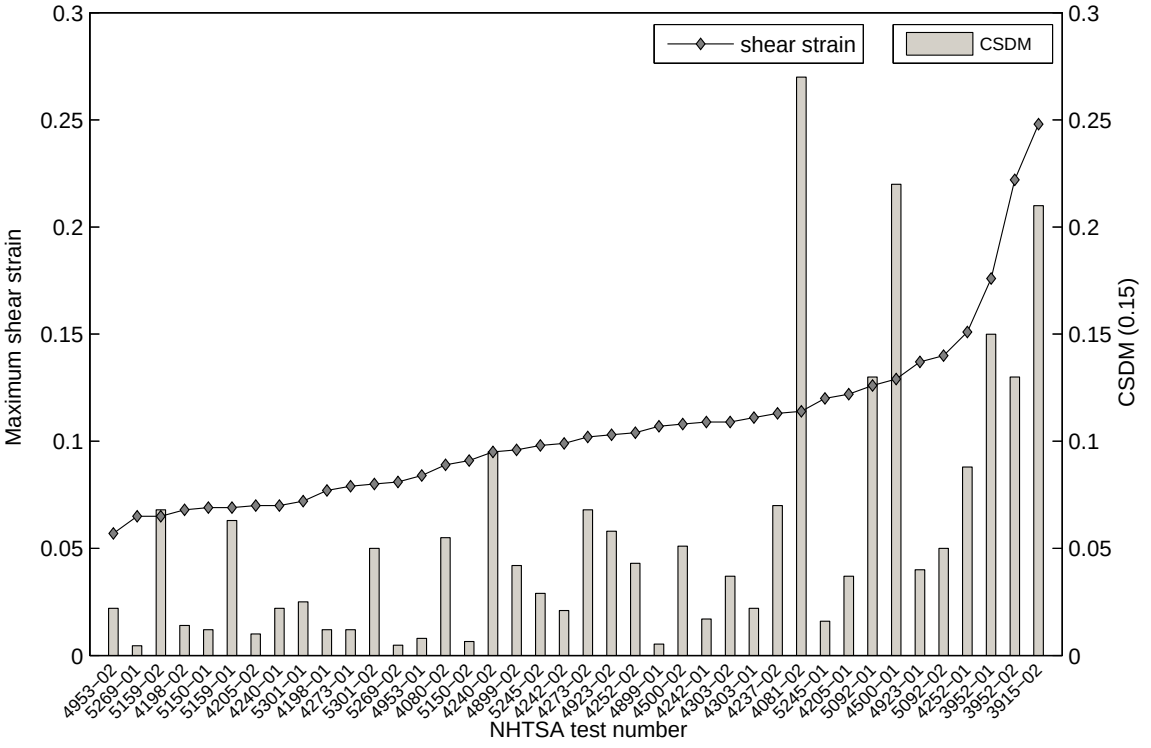

Figure 3: Comparison of the maximum shear strain from the analytical model and CSDM (0.15) in SIMon.

Generally, HIC15 predicts head injury based only on linear accelerations of the head during impact, while the SIMon prediction is dominated by angular accelerations of the head. The analytical brain injury model in the sagittal plane employs the maximum shear strain as the injury indicator of DAI. The maximum shear strain from the analytical model varies more closely with the combination of relative magnitudes of both linear and angular head kinematics. It is consistent with the structural coupling between the rotation and translation of the brain. The relatively small range of maximum shear strain coheres with the nearly same impact speed and with the relatively small range of head kinematics for all of the tests.

DISCUSSION

In this work, an analytical brain injury model with a simple strain measure was developed based on the assumption that the relative translation and rotation of the brain with respect to the skull are coupled. Bayly et al. (2005) studied strain deformation in human volunteers under occipital deceleration impact using magnetic resonance imaging. They concluded that angular acceleration of the skull was not required to cause angular acceleration of the brain due to the tangential components of tethering forces, which were transmitted by the vascular, neural, and dural elements, binding the brain to the base of the skull. The tangential forces changed the angular momentum of the brain, causing brain rotation. King et al. (2003) argued that only a small portion of brain motion results from linear acceleration, while the majority of brain motion is due to angular acceleration. However, no experiments under pure linear or pure angular acceleration have been conducted to study their distinctive contributions to brain motion. In addition, the patterns of relative brain motion inside the skull are not yet fully understood. Further studies will help better understand the coupling between the translation and rotation of the brain.

This study suggests that both linear and angular accelerations contribute significantly to brain injuries, although recent studies are mostly based on the assumption that angular acceleration is more injurious to the brain than linear acceleration. King et al. (2003) cited data derived from a series of experiments for determining the role of a football helmet using Hybrid III dummies. They found that linear acceleration of the dummy head was significantly reduced with a helmet on, while the reduction of angular acceleration was not as significant. Mueller (1998) reported that football helmets could greatly reduce brain injuries occurred on the football field. Comparing the experimental results with Mueller's conclusion, King et al. (2003) concluded that the mechanism of brain injury might not be related to angular acceleration as strongly as suggested by some researchers. Anderson et al. (2003) conducted a series of impact experiments on sheep to study the relationship between the axonal brain injury and the severity of impact to the head. They concluded that the most reliable correlates for the extent of injury were both linear and angular kinematics of the head. Zhang et al. (2004) also suggested that both linear and angular accelerations might be essential causes for brain injuries. In their study, a linear acceleration of 85 g with an impact duration of between 10 to 30 ms and a HIC15 value of 240 were proposed as the injury tolerance for mild traumatic brain injury. These most recent studies appear to undermine the predominant emphasis on angular acceleration causing brain injury.

Although the HIC system has been widely used and accepted as a government standard of head injury, it is evaluated only based on linear accelerations of the head, and possible injuries caused

by angular accelerations cannot be predicted. In contrast, the SIMon prediction is dominated by angular accelerations of the head. With very high linear accelerations as inputs, SIMon only yields very small possibility of brain injury in terms of all three injury metrics. This work is expected to fill the gap between existing simple models and more complex FE models for better brain injury prediction under more severe impacts. The adoption of both types of accelerations as inputs unveils some of the important features of brain injury mechanisms. Compared with several hours in FE models, only several seconds are needed to finish the computation on the analytical model for a similar simulation. This reduction in execution time without sacrifice of injury prediction capability is one of the advantages that would facilitate widespread use of this model.

The proposed measure of strain on the analytical brain injury model for DAI prediction can only capture the characteristics of brain motion/deformation in the sagittal plane. However, all the existing experiments generate three-dimensional head kinematics during impacts. For most of the experiments under frontal and rear impacts, the head kinematics in the sagittal plane are dominant. The planar model is adequate when the out-of-plane head kinematics are insignificant. For those tests that have relatively large out-of-plane measured head kinematics, the results using the planar brain injury model cannot accurately represent the severity of the impacts.

CONCLUSIONS

A simple measure of strain based on an analytical brain injury model was presented in this work for DAI prediction. The maximum shear strain was selected as the indicator of brain injury. This model was applied to low-severity impacts in Hardy et al's (2001) tests and more severe impacts in the NCAP real frontal crash tests. The HIC15 values were calculated for the frontal crash tests, which were also reconstructed in the SIMon FE head model, for purposes of comparison. The results show that the simple measure of strain has the capabilities of predicting brain injuries due to impact. The maximum shear strain from the analytical model can be used as a critical element for brain injury prediction. In general, HIC15 predicts head injury based only on linear accelerations of the head during impact, while the brain injury prediction in SIMon is dominated by angular accelerations of the head. The maximum shear strain in the analytical model varies more closely with the combination of both linear and angular head kinematics. It is consistent with the structural coupling between the rotation and translation of the brain.

REFERENCES

Alem, N. (1974). Simulation of head injury due to combined rotation and translation of the brain. In *Proceedings of the 18th Stapp Car Crash Conference*, pp. 579–598.

Anderson, R., C. Brown, P. Blumbergs, A. McLean, and N. Jones (2003). Impact mechanics and axonal injury in a sheep model. *Journal of Neurotrauma 20*, 961–974.

Bain, A. and D. Meaney (2000). Tissue-level thresholds for axonal damage in an experimental model of central nervous system white matter injury. *Journal of Biomechanical Engineering 122*(6), 615–622.

Bandak, F. and R. Eppinger (1994). A three-dimensional finite element analysis of the human brain under combined rotational and translational acceleration. In *Proceedings of the 38th Stapp Car Crash Conference*, pp. 145–163.

Bayly, P., T. Cohen, E. Leister, D. Ajo, E. Leuthardt, and G. Genin (2005). Deformation of the human brain induced by mild acceleration. *Journal of Neurotrauma 22*(8), 845–856.

Brinn, J. and S. Staffeld (1970). Evaluation of impact test accelerations: a damage index for the head and torso. In *Proceedings of the 14th Stapp Car Crash Conference*, pp. 188–220.

Centers for Disease Control and Prevention (CDC), National Center for Injury Prevention and Control (2005). Facts about traumatic brain injury.

Chu, C., M. Lin, H. Huang, and L. M. (1994). Finite element analysis of cerebral contusion. *Journal of Biomechnics 27*(2), 187–194.

Claessens, M., F. Sauren, and J. Wismans (1997). Modeling of the human head under impact conditions: a parametric study. In *Proceedings of the 41st Stapp Car Crash Conference*, pp. 315–328.

Department of Health and Human Services, Centers for Disease Control and Prevention (CDC), National Center for Injury Prevention and Control (2002). CDC injury research agenda.

DiMasi, F., R. Eppinger, and F. Bandak (1995). Computational analysis of head impact response under car crash loadings. In *Proceedings of the 39th Stapp Car Crash Conference*, pp. 425–438.

Galford, J. and J. McElhaney (1970). A viscoelastic study of scalp, brain, and dura. *Journal of Biomechanics 3*, 211–221.

Hardy, W., C. Foster, M. Mason, K. Yang, A. King, and S. Tashman (2001). Investigation of head injury mechanism using neutral density technology and high-speed biplanar x-ray. *Stapp Car Crash Journal 45*, 337–368.

Hosey, R. and Y. Liu (1982). A homeomorphic finite element model of the human head and neck. In R. Gallagher, B. Simon, P. Johnson, and J. Gross (Eds.), *Finite elements in biomechanics*, pp. 379–401. John Wiley & Sons.

Huang, H., M. Lee, W. Chiu, C. Chen, and S. Lee (1999). Three-dimensional finite element analysis of subdural hematoma. *The Journal of Trauma: Injury, Infection, and Critical Care 47*(3), 538–544.

Huang, H., M. Lee, S. Lee, W. Chiu, L. Pan, and C. Chen (2000). Finite element analysis of brain contusion: an indirect impact study. *Medical & Biological Engineering & Computing 38*(2), 253–259.

Khalil, T. and D. Viano (1982). Critical issues in finite element modeling of head impact. In *Proceedings of the 26th Stapp Car Crash Conference*, pp. 87–102.

King, A., K. Yang, L. Zhang, and D. Viano (2003). Is head injury caused by linear or angular acceleration? In *Proceedings of the 2003 IRCOBI Conference*, pp. 1–12.

Kleiven, S. (2005). Influence of direction and duration of impacts to the human head evaluated using finite element method. In *Proceedings of the 2005 IRCOBI conference*, pp. 41–57.

Low, T. (1986). Rotational head injury model - a lumped parameter approach. Master's thesis, The Ohio State University.

Margulies, S. and L. Thibault (1992). A proposed tolerance criterion for diffuse axonal injury in man. *Journal of Biomechanics 25*(8), 917–923.

Morrison III, B., H. Cater, C.-B. Wang, F. Thomas, C. Hung, G. Ateshian, and L. Sundstrom (2003). A tissue level tolerance criterion for living brain developed with an in vitro model of traumatic mechanical loading. *Stapp Car Crash Journal 47*, 93–105.

Mueller, F. (1998). Fatalities from head and cervical spine injuries occurring in tackle football: 50 years' experience. *Clinical Journal of Sport Medicine 17*(1), 169–182.

Padgaonkar, A., K. Krieger, and A. King (1975). Measurement of angular acceleration of a rigid body using linear accelerations. *Journal of Applied Mechanics 42*, 552–556.

Ruan, J., T. Khalil, and A. King (1991). Human head dynamic response to side impact by finite element modeling. *Journal of Biomechanical Engineering 113*, 276–283.

Slattenschek, A. and W. Tauffkirchen (1970). Critical evaluation of assessment methods for head impact applied in appraisal of brain injury hazard, in particular in head impact on windshield. In *International Automobile Safety Conference Compendium*, pp. 1084–1112.

Stalnaker, R., J. Fogle, and J. McElhaney (1971). Driving point impedance characteristics of the head. *Journal of Biomechanics 4*, 127–139.

Takhounts, E., R. Eppinger, J. Campbell, R. Tannous, E. Power, and L. Shook (2003). On the development of the SIMon finite element head model. *Stapp Car Crash Journal 47*, 107–133.

Thurman, D., C. Alverson, K. Dunn, J. Guerrero, and J. Sniezek (1999). Traumatic brain injury in the united states: a public health perspective. *Journal of Head Trauma and Rehabilitation 14*(6), 602–615.

Ueno, K., J. Melvin, L. Li, and J. Lighthall (1995). Development of tissue level brain injury criteria by finite element analysis. *Journal of Neurotrauma 12*, 695–706.

Ward, C. and M. Chan (1980). Intracranial pressure - a brain injury criterion. In *Proceedings of the 24th Stapp Car Crash Conference*, pp. 163–185.

Willinger, R., H. Kang, and B. Diaw (1999). Three-dimensional human head finite-element model validation against two experimental impacts. *Annals of Biomedical Engineering 27*(3), 403–410.

Young, P. (2003). An analytical model to predict the response of fluid-filled shells to impact - a model for blunt head impacts. *Journal of Sound and Vibration 267*, 1107–1126.

Zhang, L., K. Yang, and A. King (2001). Comparison of brain responses between frontal and lateral impacts by finite element modeling. *Journal of Neuratrauma 18*(1), 21–30.

Zhang, L., K. Yang, and A. King (2004). A proposed injury threshold for mild traumatic brain injury. *Journal of Biomechanical Engineering 126*, 226–236.

Zhou, C., T. Khalil, and A. King (1995). A new model comparing impact responses of the homogeneous and inhomogeneous human brain. In *Proceedings of the 39th Stapp Car Crash Conference*, pp. 121–137.

Zou, H., S. Kleiven, and J. Schmiedeler (2006). The effect of brain mass and moment of inertia on relative brain-skull displacement during low-severity impacts. In *Proceedings of 2006 International Crashworthiness Conference*.

APPENDIX

Table 3: NCAP frontal barrier crash test configuration.

NHTSA Test No.	HIC15	HIC36	Vehicle Description	Impact Speed (km/h)
5245-01	105.84	211.20	2005 Acura RL	56.33
5159-01	139.74	270.90	2005 Dodge Ram 1500	56.46
5092-02	143.59	258.73	2004.5 Volvo S40	56.20
4303-01	156.44	270.79	2003 Honda Pilot	55.91
5301-01	159.63	319.17	2005 Dodge Dakota	56.49
5150-01	173.88	306.40	2005 Nissan Altima	56.20
4242-01	178.37	300.78	2002 Honda Odyssey	56.49
5092-01	185.11	392.50	2004.5 Volvo S40	56.20
4205-02	187.55	340.36	2002 Ford Thunderbird	56.20
4273-01	193.27	341.86	2002 Mini Cooper	56.16
4080-02	214.75	365.09	2002 Ford Focus 2 Door	56.00
4198-01	220.37	362.65	2002 Saturn VUE 4 Door	56.30
5150-02	232.14	449.69	2005 Nissan Altima	56.20
5159-02	250.40	381.92	2005 Dodge Ram 1500	56.46
4252-02	256.21	485.90	2002 Dodge Dakota	56.16
5269-02	264.56	403.73	2005 Toyota Sienna	56.33
4081-02	287.26	453.90	2002 Jeep Liberty	56.30
5269-01	287.56	472.70	2005 Toyota Sienna	56.33
5245-02	288.66	395.23	2005 Acura RL	56.33
4953-02	296.35	403.09	2004 Volkswagen Touareg	56.65
4237-02	329.51	502.77	2002 Nissan Frontier	56.16
4205-01	337.31	516.35	2002 Ford Thunderbird	56.20
4303-02	341.65	466.06	2003 Honda Pilot	55.91
4240-02	343.88	495.74	2002 Dodge Ram1500	56.49
4953-01	353.03	597.10	2004 Volkswagen Touareg	56.65
4923-02	360.05	508.06	2004 Cadillac SRX	56.65
4500-02	365.45	590.17	2003 Isuzu Rodeo MPV	56.65
4242-02	366.52	454.77	2002 Honda Odyssey	56.49
4273-02	384.51	700.54	2002 Mini Cooper	56.16
4899-02	408.98	588.39	2004 Chevrolet Colorado	56.97
4240-01	414.35	656.30	2002 Dodge Ram1500	56.49
4923-01	433.12	523.10	2004 Cadillac SRX	56.65
5301-02	435.43	683.72	2005 Dodge Dakota	56.49
4198-02	524.98	770.88	2002 Saturn VUE 4 Door	56.30
3915-02	534.23	737.17	2002 Toyota Tundra	56.16
3952-01	540.79	788.00	2002 Buick Rendezvous	56.60
4899-01	544.04	778.52	2004 Chevrolet Colorado	56.97
4500-01	631.51	894.70	2003 Isuzu Rodeo MPV	56.65
4252-01	654.04	969.91	2002 Dodge Dakota	56.16
3952-02	820.82	940.66	2002 Buick Rendezvous	56.60

Table 4: Peak head angular velocities and accelerations in NCAP frontal crash tests.

NHTSA Test No.	Max Abs Ang Acc $X\left(\frac{rad}{s^2}\right)$	Max Abs Ang Acc $Y\left(\frac{rad}{s^2}\right)$	Max Abs Ang Acc $Z\left(\frac{rad}{s^2}\right)$	Max Abs Ang Vel $X\left(\frac{rad}{s}\right)$	Max Abs Ang Vel $Y\left(\frac{rad}{s}\right)$	Max Abs Ang Vel $Z\left(\frac{rad}{s}\right)$
5245-01	820.65	2473.35	876.77	12.27	30.16	6.54
5159-01	1292.23	1617.05	676.77	19.18	30.31	6.54
5092-02	1140.75	3651.32	1694.39	11.23	24.49	19.74
4303-01	940.37	1724.20	863.82	7.73	24.95	9.69
5301-01	1235.79	1874.68	1987.45	6.45	29.52	9.94
5150-01	749.90	1201.24	1369.89	7.74	19.89	7.20
4242-01	1281.71	1746.32	1305.88	12.50	24.46	14.12
5092-01	1007.02	5188.61	1226.12	5.03	25.56	7.23
4205-02	1439.23	3066.71	1833.27	11.47	20.86	12.64
4273-01	1387.70	2735.41	1749.16	12.95	18.81	12.90
4080-02	1248.71	3003.10	1851.04	9.50	23.17	30.21
4198-01	993.27	2316.92	1205.11	14.59	21.5	15.23
5150-02	1001.11	1742.03	1425.52	14.09	15.43	16.06
5159-02	863.51	1947.10	1444.66	18.04	29.78	16.17
4252-02	1658.27	2612.48	2065.49	11.23	31.1	13.85
5269-02	1455.49	1627.03	948.62	8.54	16.84	12.04
4081-02	2739.59	2340.01	2950.21	34.07	27.28	39.22
5269-01	845.78	1313.29	1702.86	11.24	14.99	18.60
5245-02	1099.03	2006.35	1378.74	15.27	24.34	19.49
4953-02	7035.63	6899.73	1561.81	9.31	19.61	26.40
4237-02	3497.97	3706.5	2684.47	15.63	39.96	18.14
4205-01	770.24	3852.77	1047.81	5.90	29.1	7.15
4303-02	1257.39	2053.04	1092.73	12.10	34.67	7.27
4240-02	1248.92	3155.89	1413.12	10.55	35.41	12.14
4953-01	821.49	1321.08	795.34	6.85	20.85	5.52
4923-02	1106.92	2071.63	1336.16	9.08	39.44	12.68
4500-02	3924.07	3815.58	1403.92	9.95	35.33	11.35
4242-02	2034.97	2186.34	2494.68	6.37	27.22	16.23
4273-02	1855.66	1877.68	2024.60	5.36	25.91	23.05
4899-02	1527.46	2573.66	1371.44	8.31	27.22	12.32
4240-01	1204.21	1893.60	1044.37	10.07	25.26	18.28
4923-01	1986.65	2386.72	1244.53	8.93	33.23	15.09
5301-02	1314.52	2814.29	1761.37	15.74	29.72	18.62
4198-02	1615.01	2200.00	1278.07	3.97	28.05	10.53
3915-02	3225.910	6796.76	2815.04	9.52	40.33	28.75
3952-01	1167.34	4077.10	1637.84	9.49	31.57	19.47
4899-01	1396.83	2004.92	1523.48	13.37	18.31	15.16
4500-01	1669.97	3466.21	2457.59	31.09	21.35	37.19
4252-01	1858.55	3299.71	1899.87	16.29	23.2	11.62
3952-02	772.13	4900.56	1884.45	5.39	35.36	22.29

Table 5: Peak head linear velocities and accelerations in NCAP frontal crash tests.

NHTSA Test No.	Max Abs Lin Acc $X\left(\frac{m}{s^2}\right)$	Max Abs Lin Acc $Y\left(\frac{m}{s^2}\right)$	Max Abs Lin Acc $Z\left(\frac{m}{s^2}\right)$	Max Abs Lin Vel $X\left(\frac{m}{s}\right)$	Max Abs Lin Vel $Y\left(\frac{m}{s}\right)$	Max Abs Lin Vel $Z\left(\frac{m}{s}\right)$
5245-01	348.45	85.18	138.00	21.52	0.86	8.70
5159-01	358.50	64.22	243.36	25.99	1.19	21.22
5092-02	386.45	129.90	194.53	21.71	4.94	11.83
4303-01	409.57	91.18	177.71	24.28	2.05	16.00
5301-01	382.96	120.28	211.27	26.08	0.96	18.91
5150-01	426.59	72.29	136.90	22.19	1.03	10.71
4242-01	429.77	141.19	118.54	23.99	3.51	13.39
5092-01	499.04	67.77	219.17	23.11	1.72	9.21
4205-02	450.91	112.01	248.74	24.69	4.71	9.66
4273-01	432.62	133.58	150.71	21.98	4.02	6.54
4080-02	475.79	148.91	257.64	23.11	6.37	8.92
4198-01	453.57	145.02	221.50	22.01	5.97	10.89
5150-02	481.4	120.90	197.62	21.62	4.64	10.33
5159-02	470.67	121.78	233.44	25.93	3.38	18.36
4252-02	453.57	135.67	259.45	28.30	6.40	15.07
5269-02	520.25	122.87	187.47	23.03	4.83	10.80
4081-02	328.54	308.99	510.25	18.28	17.79	19.12
5269-01	551.48	116.16	170.28	23.25	4.20	9.60
5245-02	464.37	175.63	302.80	21.89	6.28	18.23
4953-02	543.85	132.70	734.68	21.83	3.44	9.31
4237-02	342.52	223.95	496.50	24.69	7.20	28.33
4205-01	580.24	97.21	273.87	24.47	3.16	11.57
4303-02	473.74	66.01	400.95	25.09	1.52	24.17
4240-02	546.76	101.44	325.06	26.11	2.54	23.99
4953-01	540.16	57.02	237.16	24.17	2.45	15.91
4923-02	607.51	73.98	224.90	28.23	3.40	13.45
4500-02	530.52	111.76	485.09	27.49	1.82	24.48
4242-02	563.44	104.50	313.50	21.82	3.74	18.04
4273-02	580.69	205.92	274.98	23.44	6.72	12.54
4899-02	615.89	78.29	285.75	24.50	1.29	14.23
4240-01	568.91	78.52	295.85	26.52	2.93	20.16
4923-01	659.31	93.60	229.40	24.87	2.66	16.34
5301-02	558.71	167.98	339.45	25.74	4.29	20.71
4198-02	649.33	134.24	324.59	23.08	2.68	12.03
3915-02	1061.81	311.99	306.35	24.57	5.95	16.80
3952-01	649.53	140.98	212.70	19.76	6.86	5.48
4899-01	701.94	116.69	196.08	22.56	4.25	5.72
4500-01	693.13	370.00	262.58	18.64	10.83	7.68
4252-01	701.03	120.85	333.63	25.75	4.60	14.40
3952-02	822.49	82.57	330.80	22.33	0.84	9.86

AUTHORS INFORMATION

Hong Zou
Department of Mechanical Engineering
The Ohio State University
650 Ackerman Road, Suite 255
Columbus, OH 43202
Phone: 614-247-8411
Email: zou.26@osu.edu

James P. Schmiedeler
Department of Mechanical Engineering
The Ohio State University
228 Building 1
650 Ackerman Road, Suite 255
Columbus, OH 43202
Phone: 614-292-4577
Email: schmiedeler.2@osu.edu